

# Fracture behaviour of toughened epoxy resins cured with *N,N'*-dimethylethylenediamine

Shinkichi Murakami, Osamu Watanabe and Hiroshi Inoue

Tonen Corporation, Corporate Research and Development Laboratory,  
Carbon Fiber Project Group, Ohi-machi, Iruma-gun, Saitama 354, Japan

and Mitsukazu Ochi, Takuya Shiraishi and Masaki Shimbo

Department of Applied Chemistry, Faculty of Engineering, Kansai University,  
Yamate-cho, Suita-shi, Osaka 564, Japan

(Received 27 June 1990; revised 30 August 1990; accepted 10 September 1990)

Two series of toughened epoxy resin systems, which are models of matrix resins for use in carbon fibre reinforced plastics, were prepared. Evaluations of the cured epoxy resins, measuring fracture toughness, impact properties, tensile properties and dynamic mechanical properties were conducted. The correlations between these properties and the apparent concentration of network chains in the resins,  $\nu$ , were investigated and the fracture surfaces were examined with a scanning electron microscope. The superior toughness of these resin systems was obtained without considerable loss in modulus. Unified maximum peak was observed in the plots of Izod impact strength, where the  $\nu$  value of the cured resins was increased.

(Keywords: epoxy resins; fracture; curing)

## INTRODUCTION

Applications of carbon fibre composites in aircraft, ships, automobiles and sporting goods have increased markedly over the past few years. Thermoset polymers, in particular epoxy resins, are popular matrices for these applications. However, their characteristic brittleness promotes microcracking and debonding of composites under mechanical and thermal loading. Therefore, recent efforts have focused on the improvement of toughness and understanding of the fracture mechanism for epoxy resins and composites<sup>1-3</sup>.

The addition of a rubbery phase to the matrix resin is one of the most successful methods for the improvement of toughness<sup>4</sup>. Much attention has been paid to the addition of a carboxyl-terminated butadiene acrylonitrile elastomer (CTBN) to the epoxy resin<sup>5-9</sup>. However, the superior toughness of the rubber-modified epoxy resin was obtained only with a considerable sacrifice in modulus and glass transition temperature ( $T_g$ ).

Another approach, controlling crosslinking density to improve toughness, was also tested<sup>4,10</sup>. In this case, some improvement was noted in modulus and  $T_g$ , but an increase in toughness cannot usually be expected.

In the course of our studies to develop toughened carbon fibre reinforced plastics (CFRP) matrix resins, the direct influence of a crosslinking structure on fracture toughness and impact strength was studied by measuring the toughness of the cured resins.

## EXPERIMENTAL

### Materials

Nine epoxy formulations based on a bifunctional epoxy resin, diglycidyl ether bisphenol A (DGEBA, Epikote

828, epoxide equivalent:  $190 \pm 5$ ) and a tetrafunctional epoxy resin, tetraglycidyl diaminodiphenylmethane (TGDDM, Epikote 604, epoxide equivalent: 119), were used in this study. A bifunctional amine, *N,N'*-dimethylethylenediamine (MeEDA) and a tetrafunctional amine, ethylenediamine (EDA) were used as curing agents. Their compositions and chemical structures are shown in Table 1.

### Curing of epoxy resins

Epoxy resins were degassed at 100°C and stirred under reduced pressure. Stoichiometric amounts of hardener were then added. The hardener was quickly dissolved at 100°C and was then poured into moulds made of two glass plates and a poly(tetrafluoroethylene) spacer. The compounds were cured at 80°C for 4 h and at 180°C for 4 h. The specimens for the tests were machined from these cured epoxy resin plates.

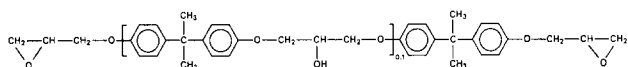
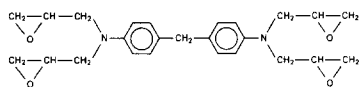
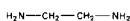
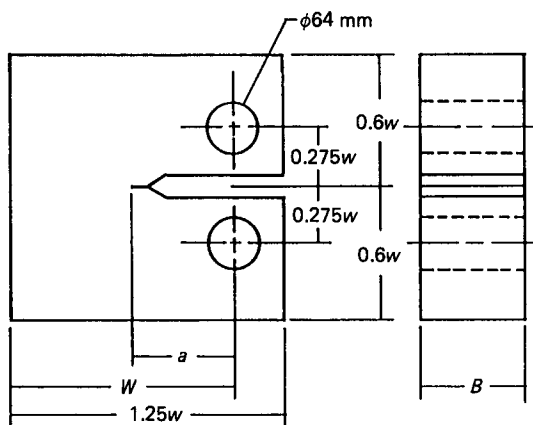
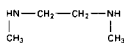
### Measurements

Dynamic mechanical properties were determined using a non-resonant forced vibration machine (Solids Analyzer RSA II, Rheometrics, Inc.) at 10 Hz, and at temperatures ranging from 20 to 250°C. Added tension was 100 g. Samples were heated at 2.0°C min<sup>-1</sup>. The test specimens, 2 mm × 3 mm × 36.7 mm, were machined from 3 mm thick cured resin plates.

The values of fracture toughness of the cured epoxy resins of samples 5 to 9 were evaluated from the critical value of the stress intensity factor,  $K_{IC}$ , for the initiation of crack growth. The fracture toughness was determined from compact tension specimens according to ASTM E 399-81. A compact tension specimen is shown in Figure 1. The thickness of the specimens was 4 mm. A sharp

**Table 1** Composition and chemical structures of resins and curing agents

Sample	Resins		Curing agents	
	DGEBA (wt%)	TGDDM (wt%)	EDA (wt%)	MeEDA (wt%)
1	0	100	0	100
2	25	75	0	100
3	50	50	0	100
4	75	25	0	100
5	100	0	0	100
6	100	0	100	0
7	100	0	75	25
8	100	0	50	50
9	100	0	25	75

**Epoxy resins**Diglycidyl ether bisphenol A (DGEBA,  $M_n = 380$ , Epikote 828)Tetraglycidyl diaminodiphenylmethane (TGDDM,  $M_n = 376$ , Epikote 604)**Curing agents**Ethylenediamine (EDA,  $M_w = 60$ )*N,N'*-Dimethylethylenediamine (MeEDA,  $M_w = 88$ )**Figure 1** Compact tension specimen for measurement of fracture toughness ( $B = 4$  mm,  $W = 27$  mm)

pre-crack was formed at the base of the slot by gently tapping a fresh razor blade in the base<sup>11</sup>. The specimen was then mounted in an Instron-type tensile machine and loaded at a constant crosshead speed ( $0.5$  mm  $\text{min}^{-1}$ ). The load,  $P$ , versus displacement curve was recorded. Schematic diagrams of the load-displacement curves of samples 6 and 7 are shown in Figure 2. They showed unstable crack propagation tendencies of a stick-slip fracturing nature.

The value of  $K_{IC}$  was calculated from:

$$K_{IC} = \frac{P}{Bw^{1/2}} f(a/w)$$

where  $P$  is the load at crack initiation,  $B$  is the thickness of the specimen,  $w$  and  $a$  are the width of the specimen and the crack length respectively, as defined in Figure 1 and  $f(a/w)$  is the geometric factor:

$$f(a/w) = \frac{(2 + a/w)(0.886 + 4.64a/w - 13.32a^2/w^2 + 14.72a^3/w^3 - 5.6a^4/w^4)}{(1 - a/w)^{3/2}}$$

Izod impact tests were conducted according to Japan Industrial Standard JIS K-6911. Dimensions of the test specimens were  $3$  mm  $\times$   $12.7$  mm  $\times$   $63.5$  mm. Notches in the specimens were machined by a notch cutter (Toyo Seiki Corp.). The fracture surfaces of the Izod specimens were observed with a scanning electron microscope (SEM-3200, Elionix Corp.) at  $10$  or  $15$  kV. Prior to the examination, the surfaces were coated with a thin layer of gold in order to improve conductivity and prevent charging.

Tensile properties were measured by an Instron-type testing machine at a crosshead speed of  $2$  mm  $\text{min}^{-1}$ , according to JIS K-6911.

**RESULTS AND DISCUSSION***Dynamic mechanical properties of cured resins*

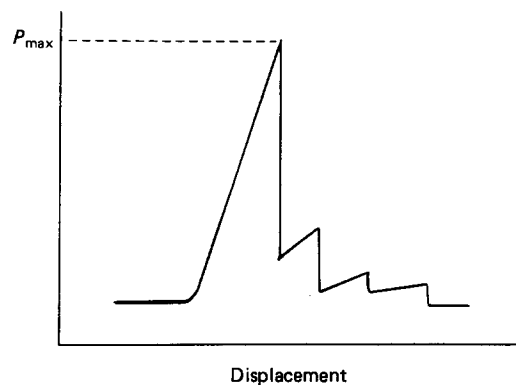
The typical spectra of the dynamic mechanical properties of cured resin systems are shown in Figure 3. The glass transition temperature,  $T_g$ , increased gradually under increased concentrations of TGDDM or EDA. This showed that crosslinking density increased and mobility of the molecular chains decreased with rises in TGDDM or EDA.

The apparent concentration of the network chains,  $\nu$ , was calculated from the equation for ideal rubber elasticity<sup>12</sup>:

$$G_r = \phi \nu RT$$

where  $G_r$  is the modulus in the rubbery region ( $40$  K above  $T_g$ ),  $\phi$  is the front factor, which is 1 for ideal rubber,  $R$  is the gas constant and  $T$  is absolute temperature. It is difficult to apply this equation exactly for epoxy resins, which are brittle materials. However, it has been successfully used by other workers<sup>12</sup> and it seems adequate for use in relative comparisons. Therefore  $\nu$  is used as a relative value in this report.

The  $\nu$  values of cured resins are listed in Table 2. The plots of  $\nu$  versus amounts of TGDDM or EDA are shown in Figure 4. As predicted,  $\nu$  increased almost linearly with

**Figure 2** Schematic diagram of load versus displacement curves of samples 6 and 7

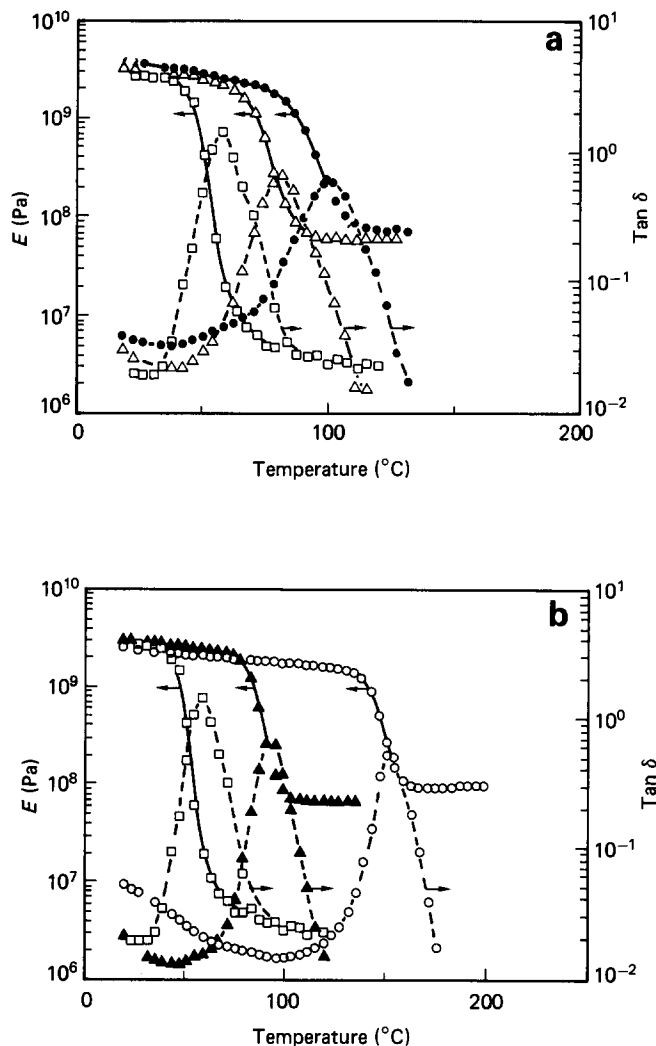


Figure 3 Dynamic mechanical properties of cured resins. (a) Samples 1 (●), 3 (Δ) and 5 (□). (b) Samples 5 (□), 6 (○) and 8 (▲)

Table 2 Properties of cured resin

Sample	Apparent concentration of network chains, $\nu$ ( $10^{-3}$ mol $\text{cm}^{-3}$ )	$T_g$ ( $^{\circ}\text{C}$ )	Izod impact strength ( $\text{kJ m}^{-2}$ )	Fracture toughness, $K_{IC}$ ( $\text{MPa m}^{1/2}$ )
1	7.0	102	9.3	—
2	6.7	100	9.7	—
3	6.2	84	12.9	—
4	4.6	67	16.1	—
5	4.0	59	3.9	$> 3.63^b$
6	8.3	154	2.9	0.74
7	7.1	117	4.7	1.18
8	6.8	94	8.6	3.63
9	5.4	70	19.2	$> 3.63^b$
ref. <sup>a</sup>	5.0	123	2.7	0.52

<sup>a</sup>DGEBA/dicyandiamide standard sample<sup>15</sup>

<sup>b</sup>Plastic deformation too large to determine

increments in either TGDDM or EDA, since the number of crosslinking points rose with increased TGDDM or EDA. The relationship between  $T_g$  of the cured resins and  $\nu$  is plotted in Figure 5. An approximately linear relationship existed between  $T_g$  and  $\nu$  in both of the resin series examined. This implies that the value of  $\nu$  is a

dominant common factor in the properties of the two resin series. This tendency agreed with MeDDM and DDM systems<sup>13,14</sup>.

Fracture toughness of cured resins

Fracture toughness at crack initiation,  $K_{IC}$  is shown in Table 2. These  $K_{IC}$  data were compared with those

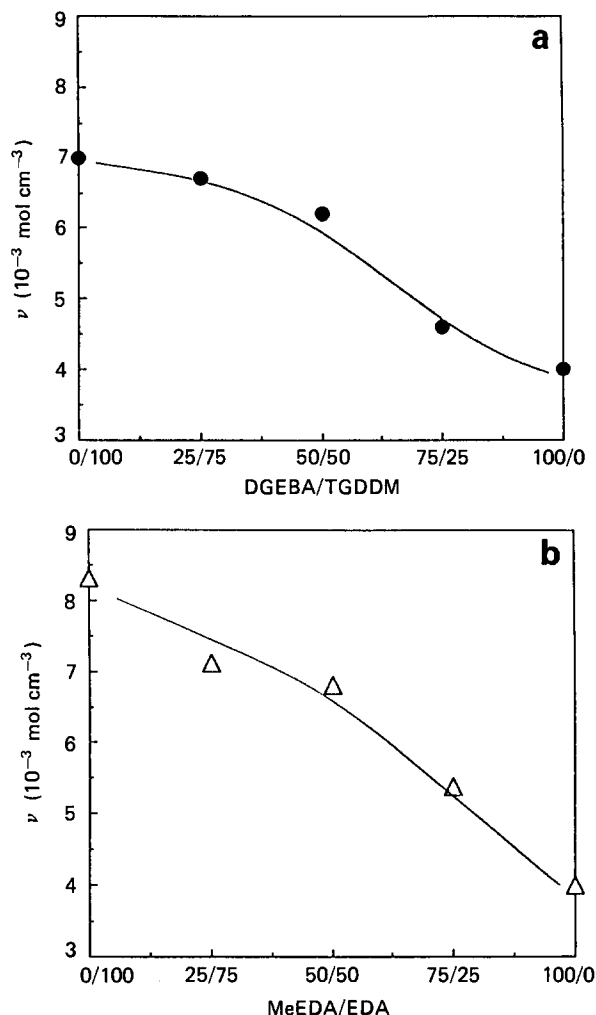


Figure 4 Apparent concentration of network chains,  $\nu$ , versus (a) DGEBA/TGDDM and (b) MeEDA/EDA

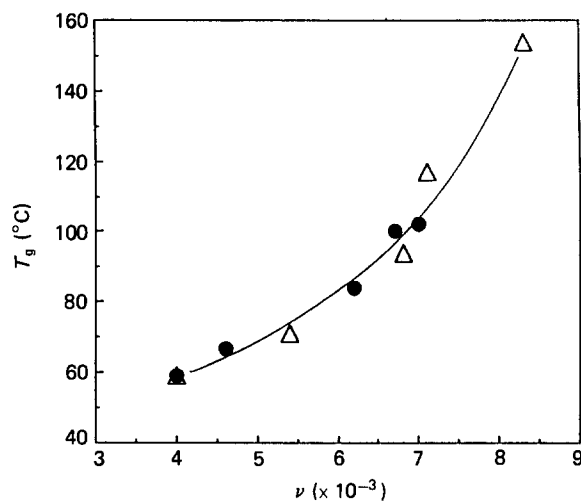


Figure 5 Glass transition temperature,  $T_g$  versus apparent concentration of network chains,  $\nu$ . Δ, MeEDA/EDA; ●, DGEBA/TGDDM

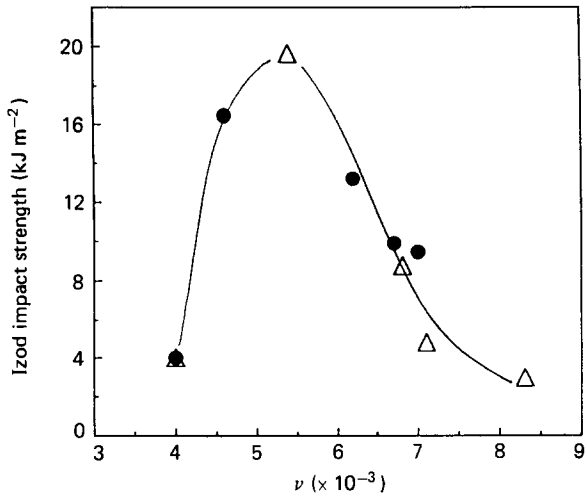


Figure 6 Izod impact strength versus apparent concentration of network chains,  $\nu$ .  $\Delta$ , MeEDA/EDA;  $\bullet$ , DGEBA/TGDDM

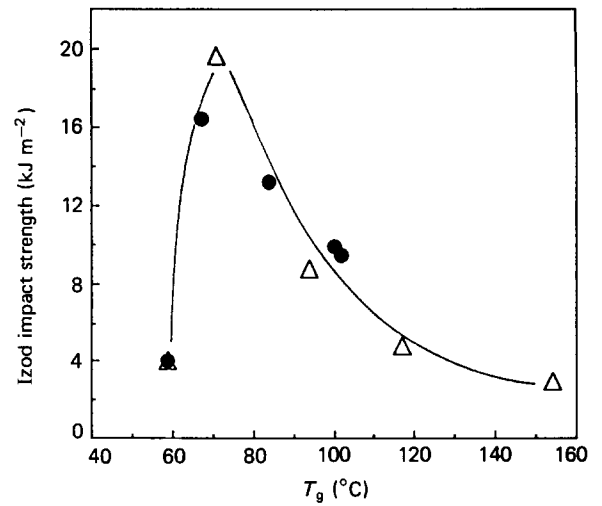


Figure 7 Izod impact strength versus glass transition temperature,  $T_g$ .  $\Delta$ , MeEDA/EDA;  $\bullet$ , DGEBA/TGDDM

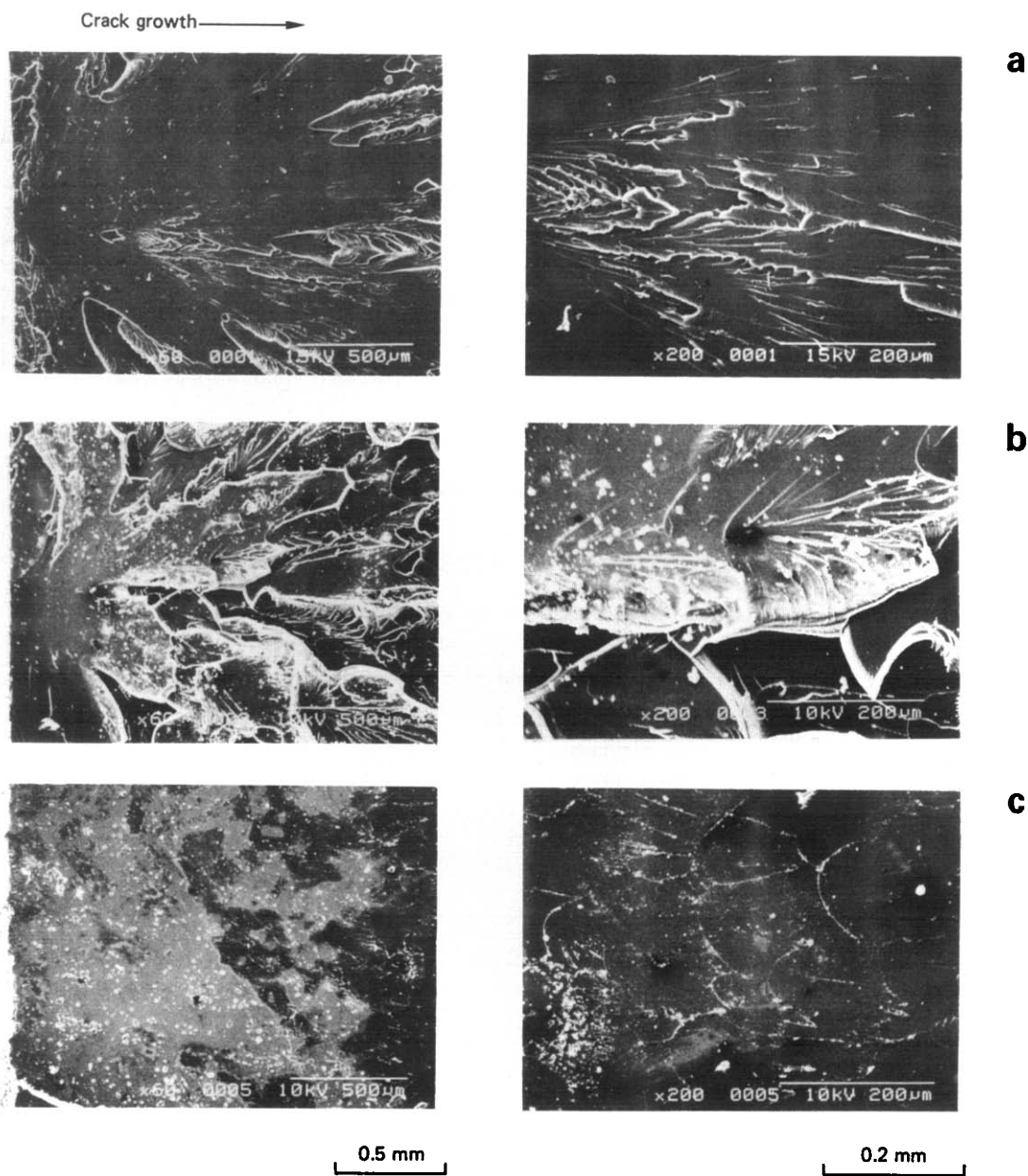


Figure 8 Scanning electron micrographs of fracture surfaces of Izod specimens. (a) Sample 1; (b) sample 3; (c) sample 5

**Table 3** Tensile properties of cured resin

Sample	Modulus (GPa)	Strength (MPa)	Fracture strain (%)
1	3.4	72	9.8
2	3.2	62	10.5
3	3.2	48	8.2
4	3.1	56	12.3
5	3.0	48	12.5
6	2.7	64	6.3
7	2.7	69	8.0
8	2.9	50	10.4
9	3.0	50	11.5
ref.	3.1	76	4.9

obtained for the dicyandiamine-cured DGEBA standard sample, which is a model resin for a typical prepreg matrix<sup>15</sup>. These samples have a much higher  $K_{IC}$  than the standard sample. This suggests that these newly developed resin systems will be tougher CFRP matrices than conventional resins.

The value of  $K_{IC}$  increased with reductions in the  $\nu$  value of the cured resins. The fracture surface of samples 6 and 7 showed stick-slip fracturing, i.e. unstable crack propagation tendencies (Figure 2). Only the  $K_{IC}$  values of samples 6 and 7, which showed stick-slip fracturing, could be evaluated. On the other hand, the fracture surfaces of samples 5, 8 and 9 showed no clear stick-slip fracturing and showed significant plastic deformation. When  $\nu$  decreased and the molecular chain length increased, the cured resin was able to endure far more plastic deformation.

#### Impact properties of cured resins

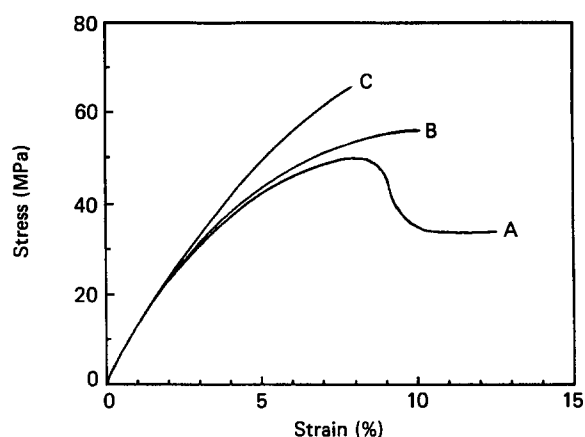
Izod impact strength is plotted versus  $\nu$  and  $T_g$  in Figures 6 and 7, respectively. Izod impact strength curves of the two resin series showed identical maximal peaks.

The increase of the impact strength with decrease in  $\nu$  of the cured resins is due to the increase in plastic deformation ability of the resins. However, the number of defects in the network structure should increase with the decrease in  $\nu$ , because the unreacted imino(-NH) groups in MeEDA form the terminal branches in the networks. The formation of defects in the networks seems to diminish strength of the cure resin. Therefore, we believe that the identical peaks of the impact strength result from the compensation of the increase in the deformation ability and in the defects of network chains.

The fracture surfaces of Izod specimens were observed under a scanning electron microscope (Figure 8). Samples 3 and 4, which revealed high impact strength, showed rougher fracture surfaces than the other samples, which showed low impact strength. It was noted that the surfaces of these samples were highly strained before catastrophic fracture. The magnitude of the roughness increased with the increasing value of  $\nu$  from sample 1 to sample 4. However, sample 5 revealed a smooth fracture surface again. The other systems (samples 6 to 9) showed similar behaviour. These results also suggest that there is an optimal crosslinking structure for impact resistance.

#### Tensile properties of cured resins

Tensile data are listed in Table 3. Most of the resins

**Figure 9** Stress-strain curves: A, sample 5; B, sample 8; C, sample 6

showed very high fracture strain, and their moduli are comparable to that of the reference sample. The typical stress versus strain curves are shown in Figure 9.

#### CONCLUSIONS

The toughening and fracture behaviour of the epoxy resins, which are matrix models for CFRP with different crosslinking structures, have been studied in detail. The following conclusions were reached: (i) a significant improvement in resin fracture toughness was achieved without sacrificing modulus; (ii) identical maximum peaks were observed in the plots of Izod impact strength with increases in the  $\nu$  value of cured resins; (iii) samples which revealed high impact strength showed rougher fracture surfaces than the other samples, which showed low impact strength.

#### REFERENCES

- Douglass, S. K., Beaumont, P. W. R. and Ashby, M. F. *J. Mater. Sci.* 1980, **15**, 1109
- Scott, J. M. and Phillips, D. C. *J. Mater. Sci.* 1975, **10**, 551
- Meeks, A. C. *Polymer* 1974, **15**, 675
- Biamant, J. and Moulton, R. J. 'Proceedings of the 29th National SAMPE Symposium, 3-5 April 1984', SAMPE, California, 1984, p. 422
- Manziona, L. T. and Gillham, J. K. *J. Appl. Polym. Sci.* 1981, **26**, 907
- Bascom, W. D., Ting, R. Y., Moulton, R. J., Riew, C. K. and Siebert, A. R. *J. Mater. Sci.* 1981, **16**, 2657
- Douglass, S. K. and Beaumont, P. W. R. *J. Mater. Sci.* 1981, **16**, 3141
- Kinloch, A. J., Finch, C. A. and Hashemi, S. *Polym. Commun.* 1987, **28**, 322
- Murakami, A., Matsushita, H., Yoshiki, T. and Shimbo, M. *J. Soc. Mater. Sci., Japan* 1985, **34**, 1099
- Murakami, A., Matsushita, H., Yoshiki, T. and Shimbo, M. *J. Adhes. Sci.* 1985, **19**, 529
- Kinloch, A. J., Shaw, S. J., Tod, D. A. and Hunston, D. L. *Polymer* 1983, **24**, 1341
- Katz, D. and Tobolsky, A. V. *J. Polym. Sci. A-2* 1964, 1595
- Murakami, S., Watanabe, O., Miyazaki, M. and Inoue, H. *Japan Patent Application*, 63-10885, 29 April 1988
- Murakami, S., Watanabe, O., Inoue, H., Ochi, M., Shiraishi, T. and Shimbo, M. 'Proceedings of the 34th National SAMPE Symposium, 8-11 May 1988', SAMPE, California, 1989, p. 2194
- Murakami, S., Watanabe, O., Miyazaki, M., Murakami, A. and Yoshiki, T. Paper 156 presented at the 37th Annual Conference of the Society of Materials Science, Kyoto, May 1988, p. 157